THE JOURNAL OF PHYSICAL CHEMISTRY B

Article

pubs.acs.org/JPCB

Molecular Insight into the Line Tension of Bilayer Membranes Containing Hybrid Polyunsaturated Lipids

Carla M. Rosetti,*[,†] Guillermo G. Montich,[†] and Claudio Pastorino[‡,§]

[†]Centro de Química Biológica de Córdoba, CIQUIBIC, Departamento de Química Biológica, Facultad de Ciencias Químicas, CONICET, Universidad Nacional de Córdoba, Ciudad Universitaria, X5000HUA, Córdoba, Argentina

[‡]Departamento de Física, Centro Atómico Constituyentes CNEA, Av. Gral. Paz 1499, 1650 San Martín, Buenos Aires, Argentina

[§]CONICET, Avda. Rivadavia 1917, C1033AAJ Cdad. de Buenos Aires, Buenos Aires, Argentina

Supporting Information

ABSTRACT: Line tension (γ) is a key parameter for the structure and dynamics of membrane domains. It was proposed that hybrid lipids, with mixed saturated and unsaturated acyl chains, participate in the relaxation of γ through different mechanisms. In this work, we used molecular dynamics simulations of the coarse-grained MARTINI model to measure γ in liquid-ordered−liquid-disordered (Lo−Ld) membranes, with increasingly larger relative proportion of the hybrid polyunsaturated lipid PAPC (4:0−5:4PC) to DAPC (di5:4PC) (i.e., X_H). We also calculated an elastic contribution to γ by the Lo−Ld thickness mismatch, tilt moduli, and bending moduli, as predicted by theory. We found that an increase in X_H decreased the overall γ value and the elastic contribution to line tension. The effect on the elastic line tension is driven by a reduced hydrophobic mismatch. Changes in the elastic constants of the phases due to an increase in X_H produced a slightly larger elastic γ term. In addition to this elastic energy, other major contributions to γ are found in these model membranes. Increasing X_H decreases both elastic and nonelastic contributions to γ. Finally, PAPC also behaves as a linactant, relaxing γ through an interfacial effect, as predicted by theoretical results. This study gives insight into the actual contribution of distinct energy terms to γ in bilayers containing polyunsaturated hybrid lipids.

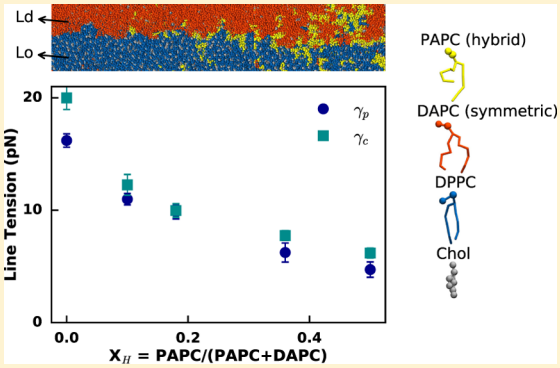

1. INTRODUCTION

Membrane domains have a line tension along their perimeter, which represents the energy cost per unit length to build up the interface. This energy is a key factor in shaping the heterogeneous surface of membranes, defining the dynamics of domain growth,[1] distribution of domain sizes,[1−3] and changes of domain shape.[3,4] Line tension has two main contributions. One is of chemical origin, due to the molecular interactions that drive lipid segregation. The other is due to local deformations of the interface between domains, to avoid hydrophobic mismatch.[5,6] A derivation of line tension based on the deformation of the bilayer via tilt and splay predicts a quadratic dependence of line tension with the hydrophobic mismatch and spontaneous curvature difference between phases.[5] To the best of our knowledge, the different contributions to line tension have not yet been independently measured in simulated or real membrane systems.

Hybrid lipids, with one unsaturated and one saturated tail,[7−12] are the most abundant in biological membranes. Several results show that hybrid lipids induce greater miscibility and lower line tension in membranes. In liquid-ordered−liquid-disordered (Lo−Ld) membranes, hybrid lipids usually trigger less segregation than their symmetric unsaturated counterparts.[12−14] In gel−fluid two-phase membranes, Szekely et al. found that replacing a symmetric lipid with a hybrid monounsaturated lipid produces a decrease in domain size, leading eventually to a completely mixed bilayer.[15] Similarly, ^{2}H NMR spectra of ternary liposomes indicate that polyunsaturated hybrids mix substantially with cholesterol in ordered domains,[16,17] in spite of the great aversion of cholesterol for polyunsaturated fatty acids.[18] There are also some simple mixtures that develop nanoscopic domains inside two-phase regions of the phase diagram,[3,14,19] several of them containing monounsaturated[14,19] or polyunsaturated[13] hybrid lipids. Compared to micron-scale domains, nanoscopic clusters increase the interface and thus the mixing between both phases. Within some theoretical frameworks, nanodomains are conceived as results of low line tension values.[8,20,21]

Different theories and experimental results have been presented regarding the effect of hybrid lipids on line tension relaxation. Several papers,[8−10] using a phenomenological model, propose that hybrid lipids behave as linactants, decreasing the melting temperature and inducing vanishing line tension away from the critical point. For large hybrid lipid

Received: October 27, 2016
Revised: January 31, 2017
Published: January 31, 2017

DOI: 10.1021/acs.jpcb.6b10836
J. Phys. Chem. B 2017, 121, 1587−1600

fractions, theory predicts that zero line tension may be achieved even close to the mixing temperature.[22] Line tension relaxes through a local effect, due to the accumulation of hybrid lipids at the interface, where they preferentially orient with the saturated tail toward the more ordered domain. Within this model, lipids have no molecular details. Molecules are actually two-dimensional (2D) entities with solely rotational degrees of freedom on the membrane plane and thus bilayer deformation is not taken into account. At the experimental level, line activity is difficult to measure, as it would require tracking the behavior of those specific molecules at the interface. Using coarse grain (CG) simulations of Lo−Ld bilayers, Schäfer et al. found that POPC (16:0−18:1PC), added at small fractions, occupied the interface and decreased line tension, but almost no effect was observed for a polyunsaturated hybrid lipid.[23] In ternary mixtures containing cholesterol, a saturated and a hybrid polyunsaturated lipid we found, using the same CG model, clusters of hybrid lipids oriented to reduce "bad" contacts of the unsaturated chain with the saturated lipid or cholesterol. In this case, the anisotropic orientation increases with the degree of unsaturation.[12] In addition to their linactant activity, it was proposed that hybrid lipids relax line tension by changing the properties of the bulk phases. Accordingly, experimental results show a clear correlation between the fraction of hybrid lipids, the hydrophobic mismatch and the domain size,[2] suggesting a role of hybrid lipids in the elastic energy component of the interfacial tension. Finally, Hassan-Zadeh et al.[24] compared ternary mixtures containing a hybrid lipid with one to four double bonds. They observed that the lower the number of unsaturations the better the partitioning in Lo domains, reducing order and compactness, and proposed that hybrid lipids reduce line tension, decreasing the compositional differences and thus the physical differences between Lo and Ld phases. A weak linactant character was recognized only for POPC and not for the polyunsaturated species, as POPC was the only one showing nanoscopic domains.[24] Nevertheless, line activity implies a reduction in line tension due to interfacial effects and will not necessarily lead to nanodomains.[22] On the other hand, the relationship between domain size and the degree of miscibility between saturated and unsaturated lipids is not always straightforward. Immiscibility regions of ternary membranes with cholesterol, sphingomyelin, and three different unsaturated lipids: DOPC (diC18:1PC), POPC, or SDPC (C18:0−C22:6PC) are similar,[25,26] but nanoscopic domains are observed only with POPC.[25,26] Ternary mixtures of POPC, cholesterol, and different saturated lipids, that is, sphingomyelin or DSPC (diC18PC), have nanoscopic domains, although the limits of the miscibility gap differ significantly.[19,25]

In this article, we address three problems that remained unclear about the actual contributions of different terms to line tension and their modulation by a hybrid polyunsaturated lipid. Our study is quantitative although the CG nature of the force field is expected to describe trends mainly at a qualitative level. Our model systems are two-phase membranes composed of 30% cholesterol, 35% saturated lipid, and 35% a mixture of hybrid (PAPC) and symmetric (DAPC) polyunsaturated lipids in variable proportions. (I) We measured the overall line tension and calculated the elastic line tension, as proposed by Kuzmin et al.,[5] as a function of the proportion of PAPC in the unsaturated lipid fraction, X_H. (II) Regarding the elastic term, we discriminated at a quantitative level the effect on the hydrophobic mismatch and on the elastic properties of the membrane. (III) We determined whether there is linactant behavior (i.e., partitioning to, and orientation at interfaces) for PAPC, as predicted by a minimal mean-field model,[22] and we further described the line activity as a function of X_H. Our results demonstrate that in Lo−Ld bilayers with polyunsaturated lipids there is, in addition to the elastic energy, a major contribution from other terms to line tension. We also observe that an increase in X_H relaxes both elastic and nonelastic terms. The elastic line tension is alleviated due to a decrease in height mismatch but not due to changes in the elastic constants of both phases. Finally, polyunsaturated hybrids exhibit linactant activity, in agreement with theoretical predictions.[22]

2. METHODS

2.1. Model and Simulation Details. We used the MARTINI (version 2.0) coarse-grained (CG) model,[27,28] with an approximate mapping of four heavy atoms per interaction site. All beads, except the first-neighbor bonded particles, interact through a Coulombic potential with a relative dielectric constant of ε_{rel} = 15, and a shifted Lennard-Jones potential, both with a cutoff at R_c = 1.2 nm. The different CG particles are classified according to their hydrophilicity.

The phospholipid's head group consists of two charged beads, modeling a phosphatidylcholine (PC) residue, and two sites of intermediate hydrophilicity, representing the glycerol−ester moiety (GL1 and GL2). We used DPPC (diC4:0PC) as a saturated lipid model with four beads per chain, the symmetric unsaturated lipid DAPC (diC5:4PC) with four double bonds per tail, and the hybrid lipid PAPC (C5:4−C4:0PC) with one tail from DPPC and the other from DAPC. For the unsaturated bonds, we followed the parametrization from refs 28 and 29. The topology of the molecules is shown in Figure S1.

Originally, we ran our simulations using the parametrization of cholesterol taken from ref 28. Recently, a new parametrization has been reported that avoids the excessive order in the liquid-ordered domains observed with the previous model.[30] We extended the simulations using the cholesterol with the improved parameters. In this work, we show the results of these extended simulations. In the Supporting Information, we present the results with both cholesterol models, showing qualitative agreement (see panel B in Figures S6−S10).

Simulations were run with GROMACS 5.0.7[31] in the *N*,*P*,*T* ensemble, with a time step of 0.03 ps. A Berendsen thermostat, with a relaxation time of 0.3 ps, was independently applied to lipids and water molecules, to fix the temperature at 300 K.[32] The bilayers were simulated in a tensionless state, applying a Parrinello−Rahman barostat with a semi-isotropic scheme, setting the average pressure to 1 bar in the *x*, *y*, and *z* directions. The parameters for the barostat in GROMACS were a coupling time constant of 2 ps and an isothermal compressibility of $\chi = 3 \times 10^{-5}$ bar^{-1}.

2.2. Details of the Physical Parameters Analyzed. *2.2.1. Intrinsic Interface and Intrinsic Profiles.* The interface between liquid phases shows thermal fluctuations that broaden the global density profiles. Profiles presented in this article were obtained after eliminating the thermal fluctuations of the interface. As shown later, these intrinsic profiles are sharper and show greater detail of the structure of the interface.

We followed a procedure similar to that described in ref 33 for interfaces between immiscible liquids. As shown in Figure 1, our membranes present two stripe domains. The direction along the domains is *y*, and the direction across the domains is *x*. Because of the periodic boundary conditions, there are two

DOI: 10.1021/acs.jpcb.6b10836
J. Phys. Chem. B 2017, 121, 1587−1600

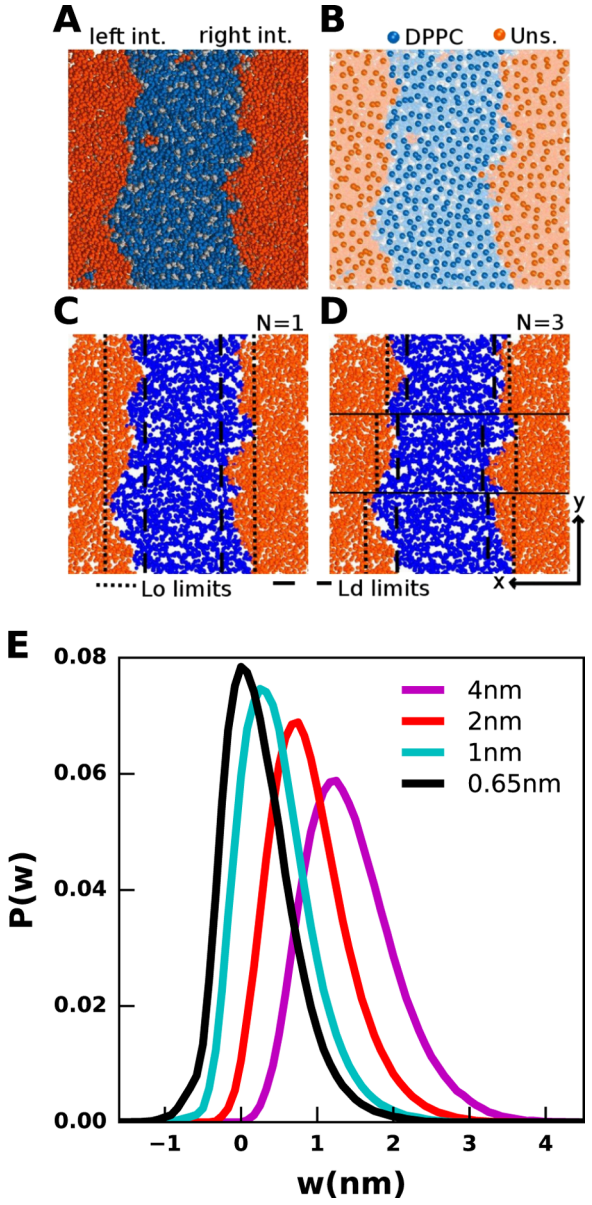

Figure 1. Procedure to define the Lo and Ld phases and to determine the position of the interfaces. (A) Snapshot of a two-phase membrane configuration with X_H = 0. DPPC is blue, DAPC is orange, and cholesterol is gray. The Lo domain, at the center, is delimited by the left and right interfaces. (B) COM of DPPC lipids (blue dots) and the unsaturated DAPC lipids (orange dots) that belong to the major Lo and Ld clusters, respectively. (C, D) DPPC lipids forming the major Lo cluster (blue), and DAPC molecules forming the major Ld cluster (orange). The vertical lines set the limits of the Lo phase (dotted lines) and Ld phase (dashed lines). (D) x is the direction across the domain, and y is the direction along the domain. The horizontal black lines divide the membrane into three slabs (i.e., N = 3), where phase boundaries are determined. The interface width (eqs 2 and 3) is calculated as the distance between the Lo and Ld phase limits, and the interface position (eq 1) is taken at the center between them. (E) Probability distribution, $P(w)$, of the interface width, w, for a slab resolution of 4−0.65 nm. For a slab of ∼0.65 nm, the peak of $P(w)$ corresponds to w = 0 nm, meaning that thermal fluctuations of the interface are largely suppressed.

infinite domains along y separated by left and right interfaces. For each configuration, we analyzed both layers independently. We first delimited both phases, by tracking the largest lipid cluster of the major components: DPPC for the liquid-ordered phase (Lo), and the unsaturated lipids, PAPC + DAPC, for the liquid-disordered (Ld) phase. A lipid was considered to belong to a cluster if its center of mass (COM) was located within a cutoff distance to it (Figure 1A,B). We found an appropriate value for this cutoff by analyzing images of both major clusters superimposed on the entire membrane for a range of cutoff lengths. We used 1.05 nm for the Lo phase and 1.35 nm for the Ld phase. Finally, the major clusters are defined by the entire set of coordinates of the sites of the lipids that belong to them. Then, the simulation box was further divided into N slabs that cross the stripe domains, with a slab width of L_y/N, L_y being the y-box length. Within each slab, the Lo domain was centered in the box (Figure 1C), and the Lo and Ld phase limits (b) were determined for both interfaces. b is defined as the cluster coordinate that protrudes more into the opposite phase (Figure 1C,D). Thus, islands of a lipid detached from this largest lipid cluster are not considered in the interface definition. The interface position (p) was calculated in each slab as

$$p_i = \frac{b_{Lo\text{-}i} + b_{Ld\text{-}i}}{2} \quad (1)$$

where subscripts Lo and Ld refer to the phase and the generic subscript i refers to the left or right interface. The interface width (w) is defined as

$$w_r = b_{Lo\text{-}r} - b_{Ld\text{-}r} \quad (2)$$

$$w_l = b_{Ld\text{-}l} - b_{Lo\text{-}l} \quad (3)$$

for the right (w_r) and left (w_l) interfaces. This procedure is repeated for different N's, and the distribution of w is obtained for each condition (Figure 1E). w decreases as the slabs are narrower. For a slab width (L_y/N) within the molecular dimensions (∼0.65 nm), the maximum of the probability distribution of w is at zero, meaning that the broadening by thermal fluctuations is largely suppressed. Profiles of density, and of other molecular properties, are computed within each slab using a binning of 0.5 nm along x. Profiles are smoother for wider slabs because they are broadened by thermal fluctuations. Upon decreasing the slab width, profiles become steeper, giving rise to an interface that is relatively sharp (see Figure S2). We used a slab resolution of 0.65 nm, and we call these profiles "intrinsic".

2.2.2. Line Tension. Line tension (γ) was calculated using two independent approaches. Taking z as the direction perpendicular to the membrane plane, γ_p was computed from the pressure tensor according to

$$\gamma_p = \frac{1}{2}(P_{per} - P_{par})L_z L_{par} \quad (4)$$

where P_{per} and P_{par} are the pressure tensor components perpendicular and parallel to the stripe domain, respectively. L_z stands for the box length in the direction perpendicular to the membrane plane, and L_{par} is the box length parallel to the domain. The factor $\frac{1}{2}$ takes into account that there are two interfaces per domain (i.e., left and right in Figure 1A). Errors were estimated from a block average analysis.[34]

We also calculated γ_c from the capillary wave spectrum of each domain boundary, traced as described before (see Intrinsic Interface and Intrinsic Profiles) according to the expression

DOI: 10.1021/acs.jpcb.6b10836
J. Phys. Chem. B 2017, 121, 1587−1600

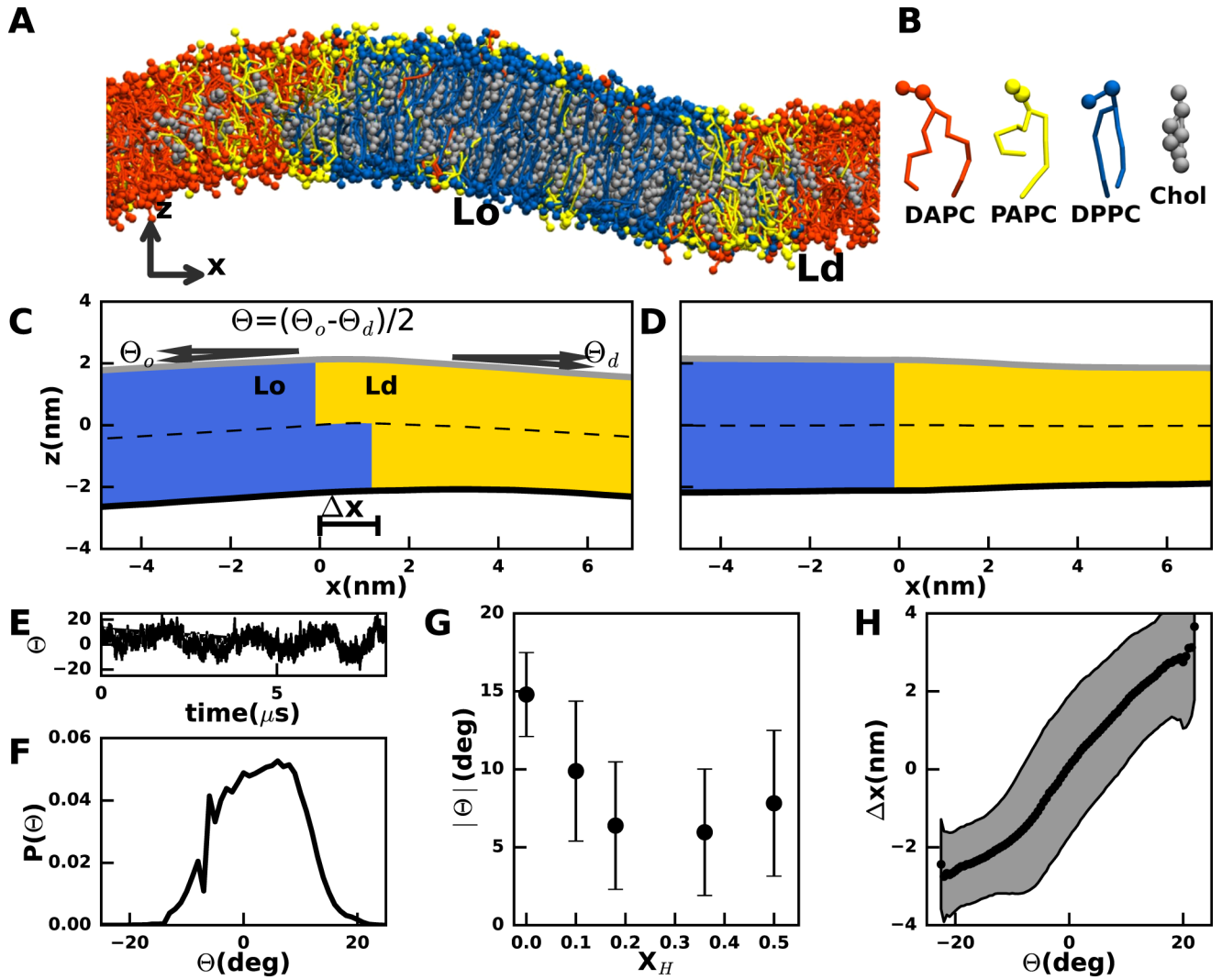

Figure 2. (A) Snapshot of a membrane with X_H = 0.36 and box size ~28 × 12 nm^2, showing the Lo and Ld domains separated by the left and right domain boundary interfaces. (B) Color coding of the lipids: DAPC is orange, PAPC is yellow, DPPC is blue, and cholesterol is gray. (C, D) Average position of the PO4 groups of the top (gray) and bottom (black) leaflets, for a Θ angle of 7° (C) or 0° (D). A positive Θ value corresponds to an upward (convex) deflection as that in C. The dashed line is calculated as the average position between PO4 groups from top and bottom leaflets. The Lo domain is depicted in blue and Ld domain in yellow. Δx is the average distance between the lower and upper interfaces. (E) Θ angle as a function of time for a X_H = 0.36 bilayer. (F) Probability distribution of Θ angles calculated from the timeline shown in E. (G) |Θ| ± sd as a function of X_H. (H) The gray region encloses the Δx ± sd values, as a function of Θ, and average Δx values are represented with black dots.

$$\gamma_c = 2\left(\frac{k_B T}{L_{par} k^2 \langle |h(k)|^2 \rangle}\right) \tag{5}$$

where $k = \frac{n2\pi}{L_{par}}$ is the wavenumber corresponding to mode n and $\langle |h(k)|^2 \rangle$ is the ensemble average of the Fourier power spectrum for the wavenumber k. k_B is the Boltzmann constant, and T is the absolute temperature. The factor 2 considers two hemilayers per interface. For membrane patches of ~20 nm × 20 nm, we averaged modes 2−5, representing fluctuations on a length scale range of [10:4 nm]. For simulation boxes of ~28 nm × 12 nm, we averaged modes 2 and 3, sampling fluctuations on a range of [6:4 nm]. To estimate the errors, equilibrium trajectories were divided into ~500 ns blocks. Averages were uncorrelated for that time lapse.

2.2.3. Line Excess. We calculated the line excess (Γ) concentration at the interface using a one-dimensional analog of the surface excess.[35] Γ_i is defined as the difference between the real number of molecules per unit length of component i in the entire system, and the number of molecules per unit length that would be present if bulk densities were maintained up to a one-dimensional Gibbs dividing line (GDL). Γ_i values were measured over intrinsic density profiles according to

$$\Gamma_i = \frac{n_{it} - L_{par}(\delta_{id} L_d^{GDL} - \delta_{io} L_o^{GDL})}{L_{par}} \tag{6}$$

where L_o^{GDL} and L_d^{GDL} are the distances from a reference position in the bulk of the Lo or Ld phase to the GDL. n_{it} is the total number of molecules of component i from the reference position at the Lo phase to the reference position at the Ld phase. δ_{io} and δ_{id} are the Lo and Ld surface densities of component i, respectively. L_{par} stands for the average box length along the domain direction. The line excess, as such, depends on the location of the GDL, whereas the relative excess of one component with respect to another is independent of the GDL position. Here, we measured Γ for the unsaturated lipids, PAPC

DOI: 10.1021/acs.jpcb.6b10836
J. Phys. Chem. B 2017, 121, 1587−1600

and DAPC, with respect to the sum of the major Lo lipids: DPPC + cholesterol. We first located GDL in such a way as to make Γ equal to zero for DPPC + cholesterol, and then calculated Γ for DAPC and PAPC relative to that line. Errors were computed from uncorrelated time blocks of 1 μs.

2.2.4. Calculation of Average Bulk Properties. Bulk-phase values were calculated from the intrinsic property profiles. Profiles show changes in the interfacial region and eventually a plateau, when reaching the bulk. We defined 2 nm-wide intervals, where bulk average values were calculated (Figure 4A). Figures S11 and S12 show profiles of density and order parameters for all membrane systems, where bulk regions are highlighted. Bulk values and density profiles are averages over both domain boundary interfaces (i.e., left and right) and over both leaflets. In some cases, domain interfaces are asymmetric, differing between the upper and lower leaflets (see, e.g., Figure 2C). In this case, profiles show small differences at the interface, but bulk values are the same (Figure S13).

2.2.5. Elastic Properties. We calculated the tilt modulus (K_t) from the fluctuations in the lipid tilt angle, and the bending modulus (K_b) from the fluctuations in the splay angle between pairs of lipids, following the method described by Khelashvili et al.[36] Tilt is the angle between each lipid director vector and the membrane normal. Splay is the angle between the director vectors of a pair of lipids (see Figure S1B). The method relies on the relationship between the free energy to bend or tilt the bilayer and the splay or tilt angle distribution of lipid molecules. First, we obtain the probability distributions, $P(\alpha)$, of tilt and splay angles (α) for each molecule and molecular pairs, respectively. Then, the tilt moduli (χ_i) per lipid type, and splay moduli (χ_{ij}) for each pair of lipids, are derived from these distributions. Finally, the overall tilt (K_t), or bending modulus (K_b), is obtained after calculating the contribution of each tilt or splay term, weighted by the proportion of lipids, or lipid pairs, respectively. The director vector for the phospholipids was defined as the vector connecting the geometrical center of beads PO4−GL1−GL2 to the geometrical center of the tail beads and, for cholesterol, as the vector from ROH to the COM of the remaining beads (Figure S1A). From the normalized probability function $\left(\frac{P(\alpha)}{\sin(\alpha)}\right)$ of tilt or splay, a potential mean function (PMF) was derived according to

$$\mathrm{PMF}(\alpha) = -kT \ln\left(\frac{P(\alpha)}{\sin(\alpha)}\right) \tag{7}$$

Then, the tilt or splay moduli were estimated from the coefficients of a quadratic function, with the generic form

$$\mathrm{PMF}(\alpha) = \frac{\chi}{2}\alpha^2 \tag{8}$$

Here, χ is used generically for χ_i and χ_{ij}, and it is the free energy necessary for tilting a lipid or splaying a pair of lipids apart, respectively. As the expression holds only for lipids with small tilt angles, the splay modulus was computed only from pairs of first-neighbor molecules in which at least one lipid is tilted by no more than 10° with respect to the bilayer normal. First-neighbors were defined as lipids sharing edges in a 2D Voronoi diagram, traced from the COM of all membrane molecules. $P(\alpha)$ are peak functions (Figure S14). The interval of angles used to fit eq 8 was taken from the mean ± sd of a Gaussian function fitted around the maximum of $P(\alpha)$. Cholesterol has two Ld populations: one perpendicular and the other parallel to the membrane normal (Figure S15).[18,29,37] In this case, we fitted tilt angles up to 30° and splay angles up to 20° to consider only those molecules oriented in the normal direction.

Finally, the membrane tilt modulus and the monolayer bending modulus were calculated as

$$\frac{1}{K_t} = \frac{1}{A_0}\frac{1}{N_t}\sum_i \frac{n_i}{\chi_i} \tag{9}$$

$$\frac{1}{k_b} = \frac{1}{N_b}\sum_{ij} \frac{n_{ij}}{\chi_{ij}} \tag{10}$$

where N_t is the total number of molecules, A_0 is the mean molecular area, and n_i is the number of molecules of type i with tilt modulus χ_i. N_b represents the total number of molecule pairs and n_{ij} the number of pairs of type ij, with splay modulus χ_{ij}. The monolayer bending modulus, k_b, is half of the bilayer bending moduls, K_b. As for the intrinsic profiles, membranes were divided into slabs and the tilt and splay angle distributions were integrated over intervals of 0.5 nm as a function of the distance to the interface position (eq 1). These angle distributions eventually converge to a single distribution upon reaching the bulk. This bulk region matches that determined using density and order properties (Figure S14). The elastic moduli were calculated from the angle distributions at the Lo and Ld bulk phases. Errors were computed from uncorrelated time blocks of 1 μs.

2.2.6. Local Membrane Thickness and Average Molecular Area. Membrane thickness was estimated as the distance between the PO4 beads of the upper and lower leaflets, along the direction normal to the membrane plane. PO4 density profiles were integrated along the domain direction (i.e., y in Figure 1). In turn, the average molecular area was calculated as the inverse of the molecular density of all lipid components, within the Lo and Ld bulk regions.

2.2.7. Order Parameters. We measured the length of the lipid director vector, calculated as described before (see Elastic Properties), along the membrane normal direction. The conformational order was estimated from the order parameter given by the average second-order Legendre polynomial of the bond angles

$$P_2(\cos(\theta)) = \left\langle \frac{1}{2}(3\cos^2(\theta) - 1) \right\rangle \tag{11}$$

where θ is the angle between each bond vector and the membrane normal. The order parameter value for the tails was averaged over all bonds between tail beads. Errors were computed from uncorrelated time blocks of 1 μs.

2.2.8. Lipid in-Plane Rotational Orientation Relative to Domain Interface. We defined a vector $\mathbf{v}_{12}$, connecting the COM of the tail bonded to the GL1 bead, which is the unsaturated tail for the hybrid lipid, to the COM of the tail bonded to the GL2 bead. The membrane is represented on the x−y plane and the domain boundary interfaces along the y direction (as in Figure 1). For the left and right domain boundaries, the interface position (eq 1) is located at $x = 0$ nm, the Ld domain at $x > 0$ nm, and the Lo domain at $x < 0$ nm. We computed the angle φ between $\mathbf{v}_{12}$, projected on the x−y plane, and y. For φ values in the range [0:180°], the saturated tail of the hybrid lipid points toward the Lo phase, and for φ angles in the interval [0:−180°], it points to the Ld phase. We computed intrinsic profiles for the orientation, φ, that were averaged over

DOI: 10.1021/acs.jpcb.6b10836
J. Phys. Chem. B 2017, 121, 1587−1600

uncorrelated time blocks of 200 ns, from which errors were calculated.

2.2.9. Overview of the Simulations. We studied two-phase membranes of three and four components, with a global composition of cholesterol/DPPC/(PAPC + DAPC) 30:35:35. We progressively increased the proportion of the polyunsaturated hybrid lipids within the unsaturated fraction, composed of a mixture of hybrid and symmetric polyunsaturated lipids $\left(X_H = \frac{\text{hybrid}}{\text{hybrid} + \text{symmetric}}\right)$, from 0 to 0.75 (i.e., X_H = 0, 0.1, 0.18, 0.36, 0.50, 0.75). For X_H = 0.75, two-phase domains were no longer observed for these box dimensions (Figure S5). Then, this membrane was not further analyzed. In a previous work, we showed that membranes with cholesterol/DPPC/PAPC (X_H = 1) present one phase with nonrandom mixing, at least up to a temperature of 270 K.[12]

Simulations were started using a previous cholesterol parametrization of the MARTINI model.[28] Bilayer patches were prepared with the same composition in both layers and a random distribution of the lipids within the membrane plane. To follow phase separation, we measured the ratio of perimeter over area (P/A) of the largest cluster of the unsaturated lipids in each bilayer frame. As the phase separation proceeds, line tension drives the minimization of the interface length, and the P/A ratio decreases. After equilibration was reached at 2−5 μs, depending on the membrane composition, the simulations were further run for several μs (insets in Figures S4 and S5). Starting from the last equilibrium configurations, we changed to the improved parametrization of cholesterol.[30] The evolution to the new equilibrium state was monitored using the P/A ratio (Figures S4 and S5), changes in the composition of PAPC at bulk (Figure S6), the relative partition of PAPC between the interface and bulk, $K_{i,b}$ (Figure S7), the line tension (Figure S8), molecular order parameters at bulk (Figure S9), and PAPC orientation at the interface (Figure S10). The analysis was performed over the last 8 μs, where all observables show that bilayers reached equilibrium. For X_H = 0, 0.1, and 0.18, we prepared 1600-lipid square patches of ∼20 nm side length. For X_H = 0.36 and 0.5, we prepared patches with 1298 lipids of ∼28 nm × 12 nm, where wider stripe domains were formed (Figure S4D,E). For those larger PAPC proportions, the compositional gradients at the interface increase (compare Figure S12 to Figure S11), and the wider simulation boxes allowed better sampling of the bulk region. With the previous cholesterol parametrization, we analyzed patches of both box dimensions (i.e., ∼20 nm × 20 nm and ∼28 nm × 12 nm) for membranes with X_H = 0.36 and 0.5. As no differences were noticed, and sampling improves in the wider patches, we used this box geometry with the newer cholesterol parameters. Representative snapshots of the membranes are shown in Figure S4.

3. RESULTS

3.1. Membranes Deform to Reduce Height Mismatch. Figure 2A shows a cut through a membrane with X_H = 0.36, with an Lo domain, rich in DPPC and cholesterol and a Ld domain, rich in the usaturated lipids DAPC and PAPC. Figure 2C,D represents membrane profiles, reconstructed from different mean values. The lipid−water interface is delimited by the profiles of the position of the PO4 groups of the outer (gray line) and inner (black line) leaflets. The distance between the PO4 groups in both leaflets correctly represents the membrane thickness. The Lo domain (blue) and the Ld domain (yellow) meet at the interface position, as defined in eq 1. The distance, Δx, represents a shift between the upper and lower domain boundary interfaces. In Figure 2A, a bending in the interface region can be noted. To characterize it, we defined the angles between the x direction and the tangent to the bulk of the Lo domain (Θ_o) or the tangent to the bulk of the Ld domain (Θ_d) (Figure 2C), with $\Theta = \frac{1}{2}(\Theta_o - \Theta_d)$. Moreover, this analysis is also used to correctly evaluate the normal direction to the membrane at the Lo and Ld domains (as explained in the Supporting Information). For illustrative purposes, we show averages over bent or flat configurations, for the same membrane containing X_H = 0.36, with Θ = 7° (Figure 2C) or Θ = 0° (Figure 2D), respectively. We assign positive Θ values to convex (upward) deflections, when going from the Lo to the Ld domain (as in Figure 2C). Time dependence of Θ angle for this bilayer is represented in Figure 2E. The corresponding angle distribution is in Figure 2F. Average absolute values, $|\Theta|$, for membranes with different compositions (i.e., X_H) do not present a monotonic tendency. They decrease until X_H = 0.2 and then present a plateau (Figure 2G). More interestingly, the distance between the upper and lower interfaces (Δx in Figure 2C) is clearly correlated with Θ. To calculate Δx, membranes are first divided into slabs that cross the domains (as in Figure 1D). Then, once the interface position is found in the upper and lower leaflets of each slab, the distance between both domain boundary interfaces, Δx, is calculated. One value is computed for each interface (i.e., left and right) in a slab. Values are then averaged over all slabs. Figure 2 H shows $\Delta x \pm$ sd values, as a function of Θ. The graph includes all pairs of values (Θ, Δx), obtained, one per interface and per frame, for all studied membrane compositions. For flat bilayers (i.e., Θ = 0°), Δx = 0 nm. Then, both interfaces are represented at the same x position in Figure 2D. In nonflat membrane configurations, instead, interfaces are shifted. In Figure 2C, domain boundaries are represented at a Δx distance of 1.3 nm, corresponding to that for Θ = 7° in Figure 2H. The bending at the interface, together with a shift between the domain boundaries in both leaflets, makes the Lo domain of the bottom layer to protrude toward the opposite Ld domain (Figure 2C). As a result, height mismatch at the water membrane plane is partially alleviated.

3.2. Line Tension as a Function of the Hybrid Lipid Proportion. The line tension between domains decreases from ∼20 to ∼5 pN, with increasing X_H (Figure 3). The values calculated from the pressure tensor (γ_p) and from capillary wave theory (γ_c) are in good agreement. The only significant difference is at X_H = 0, where γ_c have larger values than γ_p.

In membranes with X_H = 0.75, γ cannot be measured because two separated domains are not clearly defined: the membrane is either demixed or the fluctuations are too large for these box dimensions (Figure S5). γ values reported in the literature for liquid phases are between 0.1 and 10 pN.[38−43] Our results show somewhat larger γ values, although within the order of magnitude of those found in the literature. To the best of our knowledge, there are no experimental measurements of γ of Lo−Ld membranes with symmetric polyunsaturated lipids. The particularly low melting temperatures and loose packing[44,45] of these lipids, and their low miscibility with cholesterol, may result in particularly larger γ values for these mixtures.

3.3. Composition of the Bulk Phases and of the Interface Region. Intrinsic density and mole ratio profiles for X_H = 0.36 are shown in Figure 4A,B. The density profiles of DPPC and of the entire unsaturated lipid fraction cross at x = 0

DOI: 10.1021/acs.jpcb.6b10836
J. Phys. Chem. B 2017, 121, 1587−1600

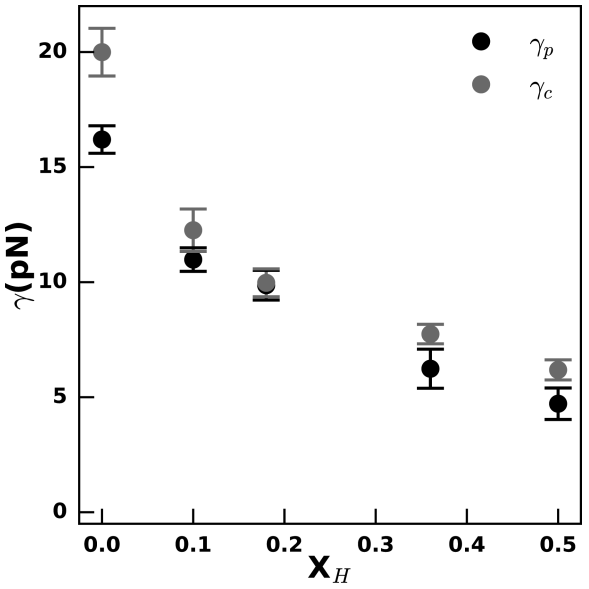

Figure 3. γ calculated from the pressure tensor (γ_p) or from capillary wave theory (γ_c), as a function of X_H.

nm, which is the interface position (eq 1), achieving an intermediate composition between both bulk phases. Around this position, density values change steeply within ∼1−2 nm. Then, the interface is defined by a sharp change in the density profiles, with a nonzero intrinsic width and, by definition, centered at x = 0 nm. Density profiles show two peaks near the interface, one for DPPC at the Lo phase side and the other for PAPC (Figure 4A), or DAPC for X_H = 0 (Figure S2), at the Ld phase side. No further density oscillations develop beyond this first layer. Cholesterol density smoothly decreases from the Lo to the Ld phase, becoming the major lipid at the interface (Figure 4A). These cholesterol molecules intercalated between domains are evidenced as a peak in the cholesterol mole ratio curve (see Figure 4B, at x = 0 nm). The two different unsaturated lipids present changes in their relative proportion within the Ld phase, as a function of the distance to the interface position: PAPC density increases toward the interface and extends further into the Lo phase, whereas DAPC is depleted from the domain boundary (Figure 4A,B).

The composition of the bulk phases is shown in Figure 4C. The Lo phase is mostly composed of DPPC and cholesterol in an approximate ratio of 1.3:1. DAPC is virtually insoluble in the Lo phase, whereas PAPC partitions up to a mole fraction of ∼8%. The Ld phase is mainly composed of DAPC (for X_H = 0), or a mixture of DAPC and PAPC, with the hybrid lipid exhibiting large solubility into the Ld domains. As PAPC replaces DAPC, the Ld phase accepts higher ratios of DPPC and cholesterol. As a result, compositional differences between phases decrease with increasing X_H, as previously described for mixtures with a different hybrid polyunsaturated lipid.[46] Lo−Ld mole fraction differences are smaller for cholesterol, DPPC, and

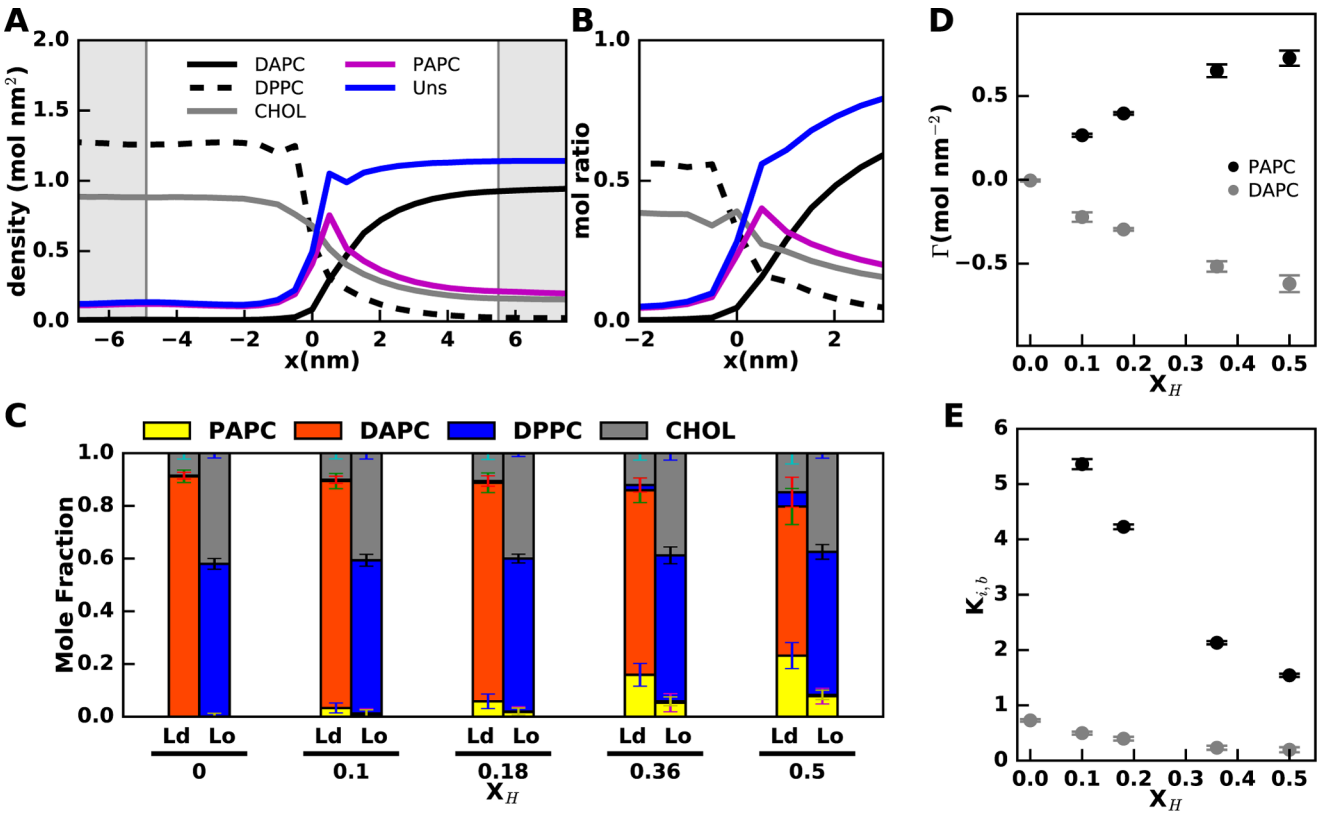

Figure 4. Mole density (A) and mole ratio (B) intrinsic profiles, averaged over both leaflets, for cholesterol, DPPC, DAPC, PAPC, and the sum of both unsaturated lipids (i.e., DAPC + PAPC) for X_H = 0.36. Negative x values correspond to the Lo domain and positive values to the Ld phase. The shadowed regions indicate the 2 nm-long intervals over which the Lo and Ld bulk values were calculated. (C) Mole fraction of the individual lipids in the Lo and Ld bulk phases, as a function of X_H. (D) Line excess (Γ) at the Gibbs dividing interface for the unsaturated lipids, DAPC, and PAPC. (E) Partition coefficient, $K_{i,b}$, for PAPC and DAPC between the the first nm of the Ld phase adjacent to the interface position (i.e., $x \in [0{:}1$ nm$]$) and the Ld bulk phase. The legend is the same for graphs A and B, and for graphs D and E.

DOI: 10.1021/acs.jpcb.6b10836
J. Phys. Chem. B 2017, 121, 1587−1600

also for the unsaturated lipid fraction: DAPC + PAPC (Figure S16).

To follow compositional changes at the interface, we calculated the line excess (Γ) of DAPC and PAPC (Figure 4D). We also studied a region of ∼1 nm of Ld phase adjacent to the domain boundary (i.e., $x \in [0{:}1\ \text{nm}]$). We delimited a 1 nm region, considering that this is the approximate diameter of one Ld−lipid molecule. We measured the composition over that area and computed the partition coefficient of PAPC and DAPC between that interfacial region and the Ld bulk phase ($K_{i,b}$) (Figure 4E). Positive Γ values mean that PAPC is relatively enriched at the interface. Negative values indicate that DAPC is less concentrated at the interface than at the bulk.The affinity of PAPC for the interface is larger at the lowest PAPC proportions, and then decreases, as evidenced by $K_{i,b}$ values (Figure 4E). The concentration of DAPC, up to X_H = 0.36, decreases preferentially from the interface, leading to negative Γ_{DAPC} and $K_{i,b} < 1$ (Figure 4D,E). Above X_H = 0.36, $K_{i,b}$ remains relatively constant, indicating that DAPC decreases at the same rate from the bulk and interface. As X_H increases, the interface composition is progressively enriched in PAPC and DPPC, and depleted of DAPC (Figure S17).

3.4. Molecular Orientation at the Interface. Our results show that lipids develop orientational order at the interface (Figure 5). For symmetric DPPC and DAPC located at the interface position (eq 1), the vector connecting the COM of both tails is preferentially oriented parallel to the domain boundary (Figure 5B). PAPC, instead, is preferentially perpendicular to the interface, with its unsaturated tail toward the Ld phase (Figure 5A). Upon increase of X_H, the interfacial orientational order is progressively lost for the symmetric and the hybrid phospholipids (Figure 5A,B). The anisotropic orientation of PAPC persists up to 2−4 nm from the interface position (not shown), probably due to gradients of DAPC and DPPC in the same region (see Figure 4A). For the symmetric lipids, however, anisotropy is mostly confined to the first molecular layer next to the domain boundary (not shown).

3.5. Order Parameters of Bulk Phases: Packing and Elastic Properties. Kuzmin et al.[5] proposed an expression for the line tension, considering that it arises from the elastic deformation of the membrane to avoid hydrophobic mismatch. In that model, the line tension depends on the Lo−Ld thickness mismatch and on the elastic properties of the phases. Here, we show that an increase in X_H reduces the differences in thickness and elastic properties between domains, by inducing disorder in the Lo phase and order in the Ld phase. Finally, we calculate the elastic line tension term for our membranes and verify that it decreases as a function of X_H.

The hydrophobic mismatch for the bilayer without PAPC (i.e., X_H = 0) is ∼0.7 nm (Figure 6A) and the Lo−Ld difference in molecular area is ∼40 Å^2 (Figure S18). Compared to ternary mixtures of DPPC/cholesterol/DOPC,[47] the height mismatch is similar, but the difference in molecular area is ∼20 Å^2 larger, as polyunsaturated acyl chains occupy larger areas than the monounsaturated tails of DOPC. Differences between Lo and Ld phases decrease with increasing X_H: the Lo domain becomes thinner and more expanded, and the Ld domain is increasingly thicker and compressed. Regarding the effect of larger X_H on the elastic constants (i.e., bilayer bending modulus, K_b, and tilt modulus, K_t), we observe a softening of the Lo phase, and a slight increase of rigidity in the Ld phase, resulting in more similar elastic properties (Figure 6B,C).

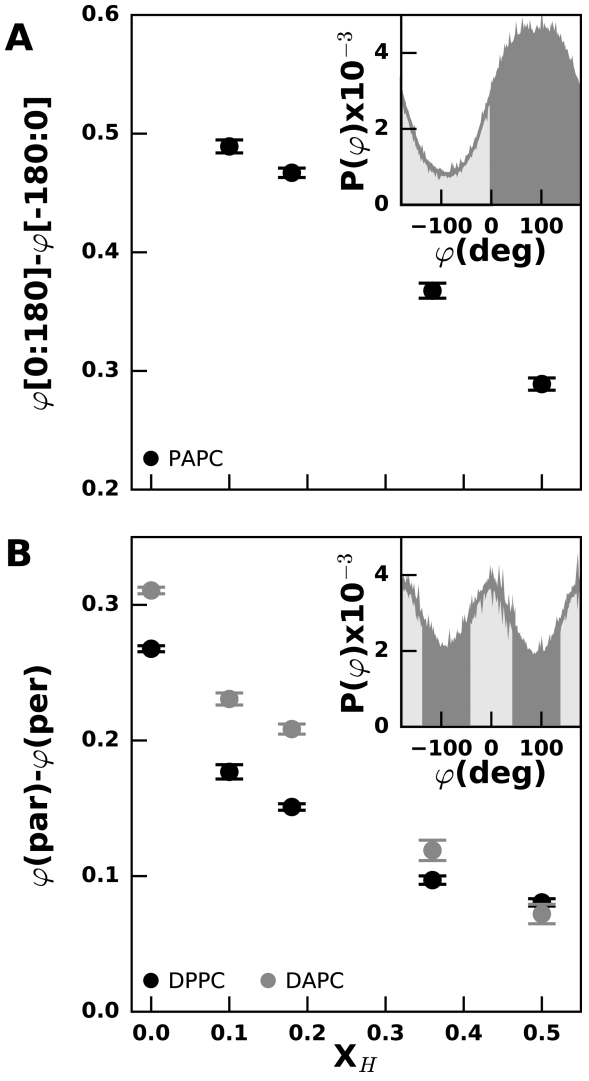

Figure 5. (A) Orientation of PAPC molecules placed at the interface position (x = 0 nm) as a function of X_H. The inset shows the probability distribution of the angle, φ, between the direction along the domain and the vector connecting the COM of the unsaturated to the saturated lipid tail. Dark gray areas correspond to orientations, where the saturated tail points to the Lo domain, and light gray regions correspond to orientations where it points to the Ld domain. We measured the difference between dark gray and light gray areas as a function of X_H. Positive values mean that PAPC shows a preferred orientation with the saturated tail pointing to the Lo phase. (B) Orientation of DPPC and DAPC lipids at x = 0 nm. We represent the difference between the probability of orientations where lipids are aligned more parallel (lighter areas in inset) and more perpendicular (darker areas in inset) to the domain boundary interface.

Lo−DPPC molecules become shorter with larger X_H (Figure 7A) and also more disordered (Figure S19A). In contrast, the lipid chains of Lo−DAPC and Lo−PAPC are progressively extended, in line with a previous study, showing that polyunsaturated tails move to the interface in more tightly packed environments[48] (Figure 7B). Within the Ld phase, we observe a stretching and ordering of DPPC lipids, but almost no changes in either unsaturated lipid, as X_H increases (Figures 7 and S19).

The tilt moduli of the different lipids (χ_i in eq 9), and the splay moduli of the different pairs of lipids (χ_{ij} in eq 10), measure the contribution of the individual membrane

DOI: 10.1021/acs.jpcb.6b10836
J. Phys. Chem. B 2017, 121, 1587−1600

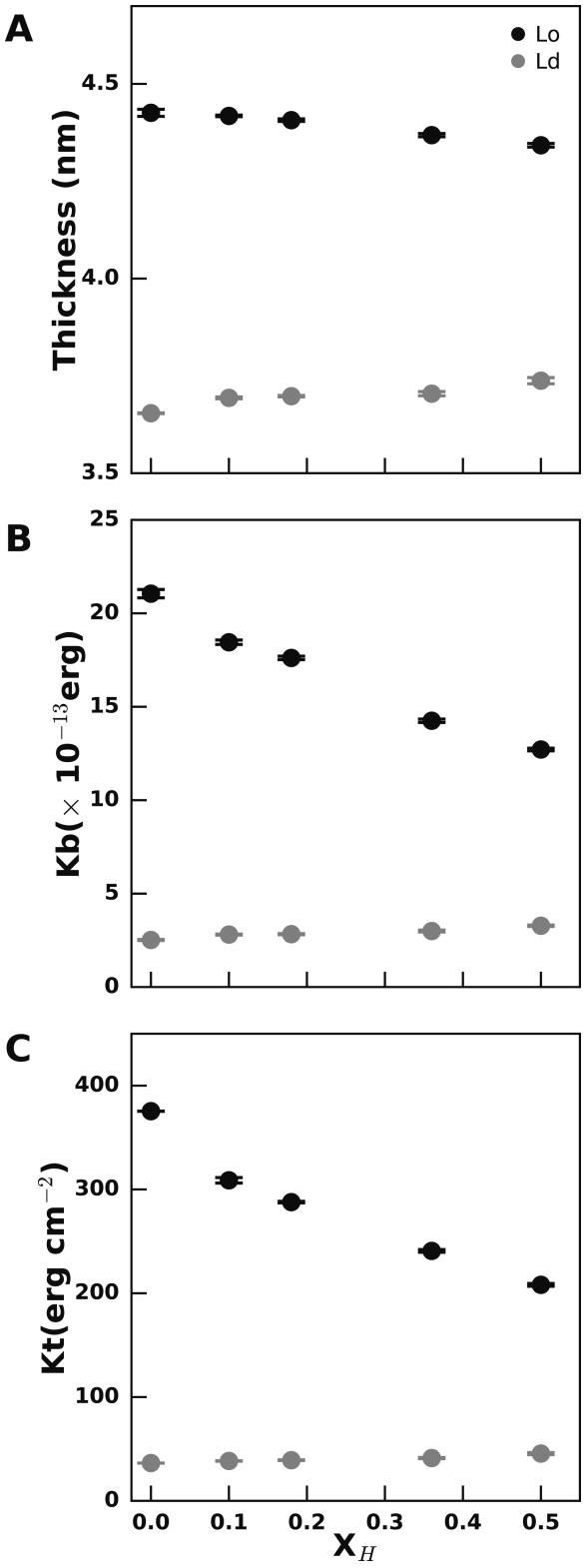

Figure 6. Thickness (A), bilayer bending modulus, K_b (B), and tilt modulus, K_t (C) of the Lo and Ld phases as a function of X_H. The legend is the same for all graphs.

components to K_t and K_b, respectively. The tilt moduli of cholesterol and DPPC decrease in the Lo phase and increase in the Ld phase, although to a lesser extent, in response to larger X_H (Figure 7C). The splay moduli of lipid pairs involving cholesterol and DPPC (i.e., DPPC–DPPC, cholesterol–cholesterol, DPPC–cholesterol) show the same trend (Figure S20A). In contrast, the tilt and splay moduli for polyunsaturated lipids remain almost unchanged with X_H in both phases, with values below 10 k_BT, and differences between Lo and Ld domains much lower than those for cholesterol and DPPC (Figures 7D and S20B,C).

According to Kuzmin et al.,[5] the line tension with origin in the elastic energy, which we will call γ_e, depends quadratically on mismatch according to

$$\gamma_e = 2^*k\left(\frac{\delta}{h}\right)^2 \tag{12}$$

with

$$k = \frac{\sqrt{K_{bo}K_{to}K_{bd}K_{td}}}{\sqrt{K_{bo}K_{to}} + \sqrt{K_{bd}K_{td}}} \tag{13}$$

where the mismatch, $\frac{\delta}{h}$, is the ratio of the thickness difference between domains in one monolayer (δ) and the average monolayer thickness (h), the subindices "o" and "d" refer to Lo and Ld phases, respectively, and the factor 2 considers both bilayer leaflets. k in eq 13 encompasses the contribution of elastic properties to γ_e. As K_t and K_b decrease, k and thus γ_e also decrease. Figure 8A shows the variation of $\frac{\delta}{h}$, k, and γ_e, as a function of X_H. In Figure 8B, we present the measured line tension values (γ_p and γ_c), and those calculated from eq 12 (γ_e), as a function of $\left(\frac{\delta}{h}\right)^2$. PAPC decreases γ_e by reducing the thickness mismatch but not through its impact on the elastic moduli (i.e., k). There is actually a slight increase in line tension, dependent on k (Figure 8A). The reason is that, as shown before, there is a softening of Lo domains but also greater rigidity of the Ld phase, which as a whole produced an increase in k. The expression for γ_e proposed by Kuzmin[5] also contains a second term, which is always negative, and reduces the line tension in bilayers where the spontaneous curvatures of both phases are different. Our calculated γ_e values are then an upper limit for the elastic line tension. Finally, the comparison of the measured γ values and γ_e shows that there is a major contribution of "nonelastic" terms to line tension. These comprise, for example, the interactions triggering the phase separation in the first place. Most importantly, both elastic and nonelastic contributions to line tension decrease with X_H (Figure 8B).

4. DISCUSSION

Our results provide insight into the dependence of several membrane properties on the relative proportion of two lipids PAPC and DAPC. Further studies with other specific systems are needed to fully explore the generality of the observed effects. Nevertheless, we repeated the analysis presented here, using other two hybrid polyunsaturated lipids: SEPC (C5:5–C5:0PC) and PLPC (C4:3–C4:0PC) at X_H = 0.18, to address preliminarily the generality of the results. We found the same trends as those for PAPC, suggesting that these could be general phenomena in the case of the increased ratio of polyunsaturated hybrid to symmetric lipids. The overall γ, and the elastic (γ_e) and nonelastic contributions to γ decrease. A reduced mismatch, and not changes in the elastic domain properties, explains the decrease in γ_e. Finally, both lipids accumulate with a preferential orientation at the interface presenting also linanctant behavior (see Figures S21–S23).

DOI: 10.1021/acs.jpcb.6b10836
J. Phys. Chem. B 2017, 121, 1587–1600

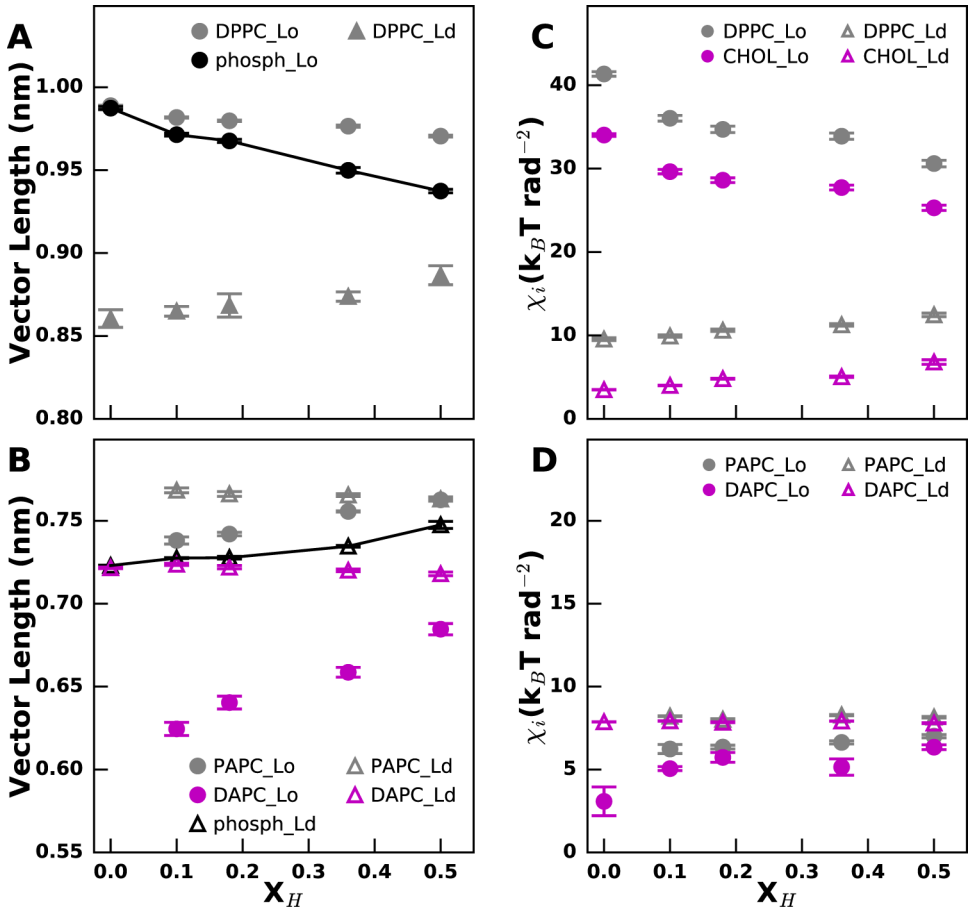

Figure 7. (A, B) Average director vector length as a function of X_H for DPPC (A), and the unsaturated lipids PAPC and DAPC (B) at the Lo and Ld phases, and for the whole phospholipid fraction at the Lo (A) and at the Ld (B) phases. The vector length value for Lo−DAPC at $X_H = 0$ (i.e., 0.4 ± 0.1) lies outside of the graph scale. Its error is particularly large and the value is probably inaccurate, due to the very small number of Lo−DAPC molecules. (C, D) Tilt modulus (χ_i) as a function of X_H for DPPC and cholesterol (C) and for the unsaturated lipids, DAPC and PAPC (D), at the Lo and Ld phases. Tilt modulus values are in k_BT units (i.e., 4.14×10^{-14} erg at 300 K). Lines are guides to the eye.

4.1. Membrane Deformation. Several results, mostly from simulations, have shown that two-phase membranes may develop different structures to compensate for the hydrophobic mismatch. For large thickness differences, antiregistered domains (Lo over Ld domains) have been reported in simulations[49,50] and real bilayers with small solid domains.[42,51] Here, thickness mismatch vanishes but a Lo−Ld interface area at the membrane midplane develops. As the domain size increases, the energetic cost due to surface tension, which scales with area, surpasses the cost due to line tension, which scales with perimeter.[52−55] This explains why model membranes with microscopic domains show coupling between leaflets.[53] On the other hand, simulated bilayers with asymmetric composition have been reported to develop curvature:[49,56] Lo domains curve inward, toward the Ld domain. Both observations can be rationalized on the basis that thickness differences manifest mostly at the terminal methyl surfaces, whereas the leaflet resists curvature at the head-group region. In our simulations, Lo domains slid over Ld domains in the opposite leaflet, and the bilayer is bent at the domain interface. Thus, the Lo domain protrudes toward the Ld phase in the opposite leaflet, and a membrane deformation would be produced at the bilayer midplane. Results from a continuum elasticity theory predict that minimum line tension is achieved at the Lo−Ld interface by shifting domain boundary interfaces in both leaflets by a few nanometers to each other.[57] In this imperfectly aligned configuration, three regions with upper−lower leaflet compositions Lo−Lo, Lo−Ld, and Ld−Ld are formed. Accordingly, the number of thickness jumps increases, but height differences in each step are smaller, reducing the deformation energy. Some of these results match our observations. Nevertheless, in our simulations, the interfaces from both leaflets were in coincidence in flat membranes, whereas a shift between boundaries was always correlated with a bend in the bilayer (Figure 2G). A more systematic study should be carried out to determine the dependence of the arrangement described on the size and shape of the simulated membrane and on line tension, to gain insight into real membranes.

4.2. Line Activity of PAPC. Safran's group has extensively studied the phase behavior of mixtures containing cholesterol, a saturated lipid, and unsaturated lipids, the latter being purely hybrids or a mixture of hybrids and symmetric unsaturated species (for a review see ref 58). Their model considers 2D amphiphiles with nearest neighbor interactions, so that any contribution from elastic energy is not considered. Our results show several similarities with their theoretical predictions regarding the phase behavior of membranes with arbitrary concentrations of hybrid lipids.[22] Below the mixing temperature (T_m), where bilayers are in a phase-separated regime, they find a transition from macroscopic domains to modulated stripe phases as the fraction of hybrids increases. Along the same compositional coordinate, but above T_m, they describe a

DOI: 10.1021/acs.jpcb.6b10836
J. Phys. Chem. B 2017, 121, 1587−1600

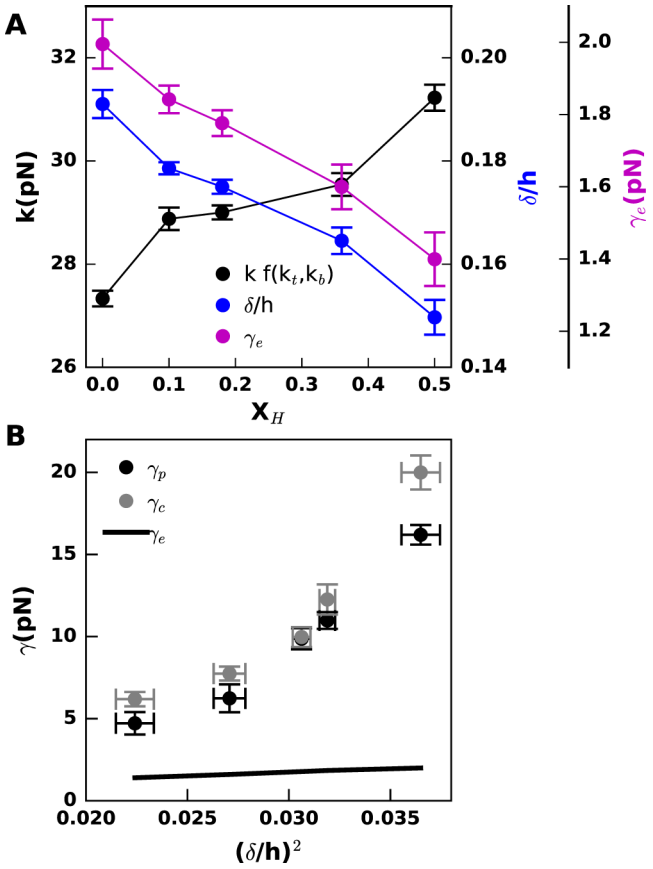

Figure 8. (A) Hydrophobic mismatch (δ/h), elastic proportionality factor (k), and elastic line tension (γ_e) (see eq 13), as a function of X_H. (B) γ_e and line tension values measured from capillary wave theory (γ_c), or from the pressure tensor (γ_p), as a function of $(\delta/h)^2$. Line tension values correspond to bilayers with X_H decreasing from 0.5 to 0, from left to right (i.e., 0.5, 0.36, 0.18, 0.1, and 0).

transition from one phase with small unstable domains to modulated fluctuations. Moreover, the critical temperatures progressively decrease with the proportion of line-active hybrids.[22] In agreement with these results, we found that bilayer mixtures developed macroscopic domains for $X_H = 0$, and membranes shifted to a one-phase regime within the range of $X_H = [0.5-1]$. This means that as X_H increases along this isothermal compositional trajectory, membranes approach and eventually cross a mixing point. Then, as theory predicts, PAPC decreases the mixing temperature in our membrane systems. In a previous work, we described the one-phase region for ternary mixtures of PAPC, cholesterol, and DPPC. We found a regime of small domains, characterized as unstable fluctuations, with PAPC showing a preferred orientation along their perimeter.[12] Decreasing the temperature to 270 K enhanced the preferred orientation of PAPC at boundaries, and domains started to develop a more organized spatial structure, within a range of a few nanometers, probably approaching a mixing point.[12] Our current results show that within the two-phase region, PAPC accumulates at the interface with the right orientation. Theory shows that this behavior, typical of a line-active molecule, reduces the line tension. Finally, the mean-field model describes the variation of different order parameter profiles at the interface, along the compositional phase space. The prediction is that the local orientation and the accumulation of hybrid lipids at the interface decrease as the membrane approaches the transition line. Coincidentally, we found that larger X_H that would drive membranes closer to the mixing point reduced the anisotropic orientation and the relative enrichment of PAPC at the interface. The predictions of the mean-field model, which includes no molecular details, are then well reproduced by our results, using a lipid model that, within its coarse level of detail, presents the spatial conformations of the atomistic lipids.[29] Nevertheless, it must be kept in mind that due to the inherent loss of degrees of freedom in CG models, enthalpy must compensate for the loss of entropy. In MARTINI, Lo−Ld phase separation is mainly triggered through differences in Lennard-Jones parameters.[59] However, properties of the already phase-separated Lo−Ld bilayers are well captured by this CG model.[60]

4.3. Effect of PAPC on the Elastic Energy Component of Line Tension. We found that PAPC makes both phases more similar to each other in terms of their composition and order parameters, as originally shown in ref 24, and regarding the elastic properties of the phases. According to Kuzmin et al.,[5] the line tension originated in the elastic energy of membrane deformation should be reduced as the thickness mismatch decreases and both phases become softer. This is summarized in eq 12. As stated previously, the full expression for the elastic contribution to line tension has a second term, which decreases γ in membranes with phases of different spontaneous curvature, and becomes zero otherwise.[5] Thus, our calculated values actually set an upper limit for γ_e. We measured a line tension relief from 2 pN down to 1.3 pN, as a function of X_H, driven by a reduction of mismatch. Smaller thickness differences are observed for larger X_H because the Ld phase becomes thicker, and the Lo domain becomes narrower. Experimental results also reported a decrease of hydrophobic mismatch in mixtures with larger ratios of hybrid lipids, using the monounsaturated POPC.[2] Nevertheless, in that case, the effect was found exclusively in the Ld phase, which became thicker, and no change was observed in the Lo phase as composition changed. Reduced mismatch, mediated by hybrid lipids, may then occur from different relative perturbations of Lo and Ld phases, depending on the lipid molecular properties. The influence of X_H on γ_e, mediated by changes in the elastic constants of both membrane phases, is less straightforward. Our results show that while the Lo phase becomes softer, decreasing line tension, the Ld phase becomes slightly less flexible for higher PAPC proportions, increasing line tension in turn. The outcome is actually a slight increase in γ_e, which depends on the effect of X_H on the elastic constants of the phases. Regarding the influence on the individual lipids, changes are mostly observed in DPPC and cholesterol. The order, length, and rigidity decreased in the Lo phase and increased in the Ld domains with larger X_H. We noticed smaller, and in some cases, negligible variations in the unsaturated lipids.

4.4. Line Tension in Hybrid-Containing Simulated Membranes: a Summary. Besides the elastic energy contribution to γ,[5,6] there are other terms giving rise to line tension.[8,61] All interactions that trigger phase separation will actually represent an energy cost at the interface. For this membrane model, there is a major contribution of those nonelastic terms to line tension. Our results showed that larger X_H reduced γ decreasing both kind of contributions simultaneously. In addition, PAPC behaves as a linactant, alleviating line tension by an interfacial effect.

Distinct molecular parameters will probably influence the relative contribution of the different mechanisms to decrease γ.

DOI: 10.1021/acs.jpcb.6b10836
J. Phys. Chem. B 2017, 121, 1587−1600

One possible determinant is the degree of unsaturation. Mean-field theory predicts that the linactant character increases with the degree of unsaturation.[11] In this regard, we expect that alleviation of γ, based on linactant-like activity, will be greater with the number of double bonds. In this line, in one-phase membranes we observed greater anisotropic orientation for the more unsaturated species in fluctuating lipid clusters.[12] On the other hand, thickness mismatch may also vary with unsaturation. Regarding pure membranes, the higher the number of lipid unsaturations, the softer and thinner the membrane becomes.[62,63] Nevertheless, it remains to be evaluated whether this actually results in greater thickness mismatch between Lo−Ld phases in mixtures containing more unsaturated lipids. Other unfavorable Lo−Ld interactions will probably also be greater for bilayers with more unsaturated species. If this is the case, the prediction will be that smaller γ values, due to smaller elastic and nonelastic terms, should be expected for the less unsaturated lipids. Linactivity, on the other hand, would be greater for polyunsaturated lipids, allowing lower line tensions at larger differences in bulk properties. In this regard, some results report Lo−Ld membranes containing polyunsaturated hybrid lipids with low line tension values. For example, ternary mixtures with the highly polyunsaturated hybrid lipid SDPC (18:0−22:6PC), with six double bonds, have macroscopic domains, as in the case of mixtures with DOPC with two monounsaturated tails. Nevertheless, SDPC-containing mixtures enter a nanoscopic domain regime, after the addition of smaller fractions of POPC, pointing to lower γ, in spite of the polyunsaturated character.[26] Results from ref 24 show that ternary mixtures with a PC, having two double bonds (16:0−18:2PC), form macroscopic domains. γ is smaller in these membranes than in mixtures with DOPC, though thickness mismatch, measured from molecular dynamic simulations, is larger.

5. CONCLUSIONS

Using molecular-dynamics simulations of the CG MARTINI model, we measured different contributions to the line tension in two-phase, liquid-ordered−liquid-disordered (Lo−Ld) membranes as a function of the relative proportion of PAPC, a hybrid polyunsaturated lipid, to DAPC (X_H). Our results show that increasing X_H decreases the overall line tension value. Eventually, the phase behavior goes from a two-phase to a one-phase regime. We further calculated the elastic energy contribution to line tension, dependent on hydrophobic mismatch, as proposed in Kuzmin et al.[5] This value decreases with higher X_H. The reason for this is a reduced hydrophobic mismatch: the Ld phase becomes thicker and the Lo phase becomes thinner. The effect on the elastic properties of both phases shows opposite trends: the Lo domain becomes softer, but the Ld domain becomes slightly less flexible. The outcome is that, through its impact on the elastic domain properties, a raise in X_H slightly increases the elastic line tension. Other contributions, besides the elastic energy, are found to be major components of the line tension value in this membrane model. More importantly, both elastic and nonelastic terms decrease as a function of X_H. Finally, we observe linactant behavior for PAPC, in agreement with predictions of a pioneer mean-field model, which included no molecular details.[58] This is particularly true as regards the dependence of the orientation and accumulation of PAPC at the interface with the fraction of hybrid lipids. We further expect that different molecular properties, such as the degree of unsaturation, will modify the relative influence of hybrid lipids on line tension through these different mechanisms.

■ ASSOCIATED CONTENT

Supporting Information

The Supporting Information is available free of charge on the ACS Publications website at DOI: 10.1021/acs.jpcb.6b10836.

Scheme of the lipid topology; density profiles using two different slab widths; normal membrane direction; equilibration of the simulations: time evolution of different physical observables; determination of the bulk phase; Lo to Ld composition difference; composition at the interfacial region; mean molecular area; configurational order parameter; splay modulus; cholesterol tilt; comparison to other hybrid polyunsaturated lipids; 23 figures (PDF)

■ AUTHOR INFORMATION

Corresponding Author

*E-mail: carla@mail.fcq.unc.edu.ar. Phone: +54 351 5353855 int 3445. Fax: +54 351 5353406.

ORCID

Carla M. Rosetti: 0000-0002-0733-2935

Notes

The authors declare no competing financial interest.

■ ACKNOWLEDGMENTS

The CONICET (PIP 112 201101004 64), MINCyT (PICT-E 134-2014, PICT 1887-2011), and SECyT-UNC are gratefully acknowledged for financial support. We also thank the CNEA (INN-CNEA 2011) for support and computer power resources.

■ REFERENCES

(1) García-Sáez, A. J.; Chiantia, S.; Schwille, P. Effect of Line Tension on the Lateral Organization of Lipid Membranes. *J. Biol. Chem.* **2007**, *282*, 33537−33544.

(2) Heberle, F. A.; Petruzielo, R. S.; Pan, J.; Drazba, P.; Kučerka, N.; Standaert, R. F.; Feigenson, G. W.; Katsaras, J. Bilayer Thickness Mismatch Controls Domain Size in Model Membranes. *J. Am. Chem. Soc.* **2013**, *135*, 6853−6859.

(3) Konyakhina, T. M.; Goh, S. L.; Amazon, J.; Heberle, F. A.; Wu, J.; Feigenson, G. W. Control of a Nanoscopic-to-Macroscopic Transition: Modulated Phases in Four-Component DSPC/DOPC/POPC/Chol Giant Unilamellar Vesicles. *Biophys. J.* **2011**, *101*, L8−L10.

(4) Stanich, C. A.; Honerkamp-Smith, A. R.; Putzel, G. G.; Warth, C. S.; Lamprecht, A. K.; Mandal, P.; Mann, E.; Hua, T.-A. D.; Keller, S. L. Coarsening Dynamics of Domains in Lipid Membranes. *Biophys. J.* **2013**, *105*, 444−454.

(5) Kuzmin, P. I.; Akimov, S. A.; Chizmadzhev, Y. A.; Zimmerberg, J.; Cohen, F. S. Line Tension and Interaction Energies of Membrane Rafts Calculated from Lipid Splay and Tilt. *Biophys. J.* **2005**, *88*, 1120−1133.

(6) Akimov, S. A.; Kuzmin, P. I.; Zimmerberg, J.; Cohen, F. S.; Chizmadzhev, Y. A. An Elastic Theory for Line Tension at a Boundary Separating Two Lipid Monolayer Regions of Different Thickness. *J. Electroanal. Chem.* **2004**, *564*, 13−18.

(7) Brewster, R.; Safran, S. A. Line Active Hybrid Lipids Determine Domain Size in Phase Separation of Saturated and Unsaturated Lipids. *Biophys. J.* **2010**, *98*, L21−L23.

(8) Brewster, R.; Pincus, P. A.; Safran, S. A. Hybrid Lipids as a Biological Surface-Active Component. *Biophys. J.* **2009**, *97*, 1087−1094.

DOI: 10.1021/acs.jpcb.6b10836
J. Phys. Chem. B 2017, 121, 1587−1600

(9) Palmieri, B.; Safran, S. A. Hybrid Lipids Increase the Probability of Fluctuating Nanodomains in Mixed Membranes. *Langmuir* **2013**, *29*, 5246−5261.
(10) Yamamoto, T.; Brewster, R.; Safran, S. A. Chain Ordering of Hybrid Lipids Can Stabilize Domains in Saturated/Hybrid/Cholesterol Lipid Membranes. *Europhys. Lett.* **2010**, *91*, No. 28002.
(11) Yamamoto, T.; Safran, S. A. Line Tension Between Domains in Multicomponent Membranes Is Sensitive to Degree of Unsaturation of Hybrid Lipids. *Soft Matter* **2011**, *7*, 7021−7033.
(12) Rosetti, C.; Pastorino, C. Comparison of Ternary Bilayer Mixtures with Asymmetric or Symmetric Unsaturated Phosphatidylcholine Lipids by Coarse Grained Molecular Dynamics simulations. *J. Phys. Chem. B* **2012**, *116*, 3525−3537.
(13) Filippov, A.; Orädd, G.; Lindblom, G. Domain Formation in Model Membranes Studied by Pulsed-Field Gradient-NMR: The Role of Lipid Polyunsaturation. *Biophys. J.* **2007**, *93*, 3182−3190.
(14) Heberle, F. A.; Wu, J.; Goh, S. L.; Petruzielo, R. S.; Feigenson, G. W. Comparison of Three Ternary Lipid Bilayer Mixtures: FRET and ESR Reveal Nanodomains. *Biophys. J.* **2010**, *99*, 3309−3318.
(15) Szekely, O.; Schilt, Y.; Steiner, A.; Raviv, U. Regulating the Size and Stabilization of Lipid Raft-Like Domains and Using Calcium Ions as Their Probe. *Langmuir* **2011**, *27*, 14767−14775.
(16) Shaikh, S. R.; Kinnun, J. J.; Leng, X.; Williams, J. A.; Wassall, S. R. How Polyunsaturated Fatty Acids Modify Molecular Organization in Membranes: Insight From NMR Studies of Model Systems. *Biochim. Biophys. Acta* **2015**, *1848*, 211−219.
(17) Williams, J. A.; Batten, S. E.; Harris, M.; Rockett, B. D.; Shaikh, S. R.; Stillwell, W.; Wassall, S. R. Docosahexaenoic and Eicosapentaenoic Acids Segregate Differently Between Raft and Nonraft Domains. *Biophys. J.* **2012**, *103*, 228−237.
(18) Brzustowicz, M. R.; Cherezov, V.; Caffrey, M.; Stillwell, W.; Wassall, S. R. Molecular Organization of Cholesterol in Polyunsaturated Membranes: Microdomain Formation. *Biophys. J.* **2002**, *82*, 285−298.
(19) Konyakhina, T. M.; Wu, J.; Mastroianni, J. D.; Heberle, F. A.; Feigenson, G. W. Phase Diagram of a 4-Component Lipid Mixture: DSPC/DOPC/POPC/CHOL. *Biochim. Biophys. Acta* **2013**, *1828*, 2204−2214.
(20) Amazon, J. J.; Goh, S. L.; Feigenson, G. W. Competition Between Line Tension and Curvature Stabilizes Modulated Phase Patterns on the Surface of Giant Unilamellar Vesicles: a Simulation Study. *Phys. Rev. E* **2013**, *87*, No. 022708.
(21) Amazon, J. J.; Feigenson, G. W. Lattice Simulations of Phase Morphology on Lipid Bilayers: Renormalization, Membrane Shape, and Electrostatic Dipole Interactions. *Phys. Rev. E* **2014**, *89*, No. 022702.
(22) Palmieri, B.; Grant, M.; Safran, S. A. Prediction of the Dependence of the Line Tension on the Composition of Linactants and the Temperature in Phase Separated Membranes. *Langmuir* **2014**, *30*, 11734−11745.
(23) Schäfer, L. V.; Marrink, S. J. Partitioning of Lipids at Domain Boundaries in Model Membranes. *Biophys. J.* **2010**, *99*, L91−L93.
(24) Hassan-Zadeh, E.; Baykal-Caglar, E.; Alwarawrah, M.; Huang, J. Complex Roles of Hybrid Lipids in the Composition, Order, and Size of Lipid Membrane Domains. *Langmuir* **2014**, *30*, 1361−1369.
(25) Petruzielo, R. S.; Heberle, F. A.; Drazba, P.; Katsaras, J.; Feigenson, G. W. Phase Behavior and Domain Size in Sphingomyelin-Containing Lipid Bilayers. *Biochim. Biophys. Acta* **2013**, *1828*, 1302−1313.
(26) Konyakhina, T. M.; Feigenson, G. W. Phase Diagram of a Polyunsaturated Lipid Mixture: Brain Sphingomyelin/1-Stearoyl-2-Docosahexaenoyl-Sn-Glycero-3-Phosphocholine/Cholesterol. *Biochim. Biophys. Acta* **2016**, *1858*, 153−161.
(27) Marrink, S. J.; de Vries, A. H.; Mark, A. E. Coarse Grained Model for Semiquantitative Lipid Simulations. *J. Phys. Chem. B* **2004**, *108*, 750−760.
(28) Marrink, S. J.; Risselada, H. J.; Yefimov, S.; Tieleman, D. P.; de Vries, A. H. The MARTINI Force Field: Coarse Grained Model for Biomolecular Simulations. *J. Phys. Chem. B* **2007**, *111*, 7812−7824.
(29) Marrink, S. J.; de Vries, A. H.; Harroun, T. A.; Katsaras, J.; Wassall, S. R. Cholesterol Shows Preference for the Interior of Polyunsaturated Lipid Membranes. *J. Am. Chem. Soc.* **2008**, *130*, 10−11.
(30) Melo, M. N.; Ingólfsson, H. I.; Marrink, S. J. Parameters for Martini Sterols and Hopanoids Based on a Virtual-Site Description. *J. Chem. Phys.* **2015**, *143*, 243152−243163.
(31) Spoel, D. V. D.; Lindahl, E.; Hess, B.; Groenhof, G.; Mark, A. E.; Berendsen, H. J. C. GROMACS: Fast, Flexible, and Free. *J. Comput. Chem.* **2005**, *26*, 1701−1718.
(32) Berendsen, H. J. C.; Postma, J. P. M.; van Gunsteren, W. F.; Dinola, A.; Haak, J. R. Molecular Dynamics with Coupling to An External Bath. *J. Chem. Phys.* **1984**, *81*, 3684−3690.
(33) Jorge, M.; Cordeiro, M. Intrinsic Structure and Dynamics of the Water/Nitrobenzene Interface. *J. Phys. Chem. C* **2007**, *111*, 17612−17626.
(34) Frenkel, D.; Smit, B. *Understanding Molecular Simulation*, 2nd ed.; Academic Press: San Diego, 2002.
(35) Myers, D. *Surfaces, Interfaces and Colloids. Principles and Applications*, 2nd ed.; Wiley-VCH: New York, 1999.
(36) Khelashvili, G.; Kollmitzer, B.; Heftberger, P.; Pabst, G.; Harries, D. Calculating the Bending Modulus for Multicomponent Lipid Membranes in Different Thermodynamic Phases. *J. Chem. Theory Comput.* **2013**, *9*, 3866−3871.
(37) Kučerka, N.; Marquardt, D.; Harroun, T. A.; Nieh, M.-P.; Wassall, S. R.; de Jong, D. H.; Schäfer, L. V.; Marrink, S. J.; Katsaras, J. Cholesterol in Bilayers with PUFA Chains: Doping with DMPC or POPC Results in Sterol Reorientation and Membrane-Domain Formation. *Biochemistry* **2010**, *49*, 7485−7493.
(38) Benvegnu, D. J.; McConnell, H. M. Line Tension Between Liquid Domains in Lipid Monolayers. *J. Phys. Chem.* **1992**, *96*, 6820−6824.
(39) Baumgart, T.; Hess, S. T.; Webb, W. W. Imaging Coexisting Fluid Domains in Biomembrane Models Coupling Curvature and Line Tension. *Nature* **2003**, *425*, 821−824.
(40) Baumgart, T.; Das, S.; Webb, W. W.; Jenkins, J. T. Membrane Elasticity in Giant Vesicles with Fluid Phase Coexistence. *Biophys. J.* **2005**, *89*, 1067−1080.
(41) Tian, A.; Johnson, C.; Wang, W.; Baumgart, T. Line Tension at Fluid Membrane Domain Boundaries Measured by Micropipette Aspiration. *Phys. Rev. Lett.* **2007**, *98*, No. 208102.
(42) Blanchette, C. D.; Lin, W.-C.; Orme, C. A.; Ratto, T. V.; Longo, M. L. Domain Nucleation Rates and Interfacial Line Tensions in Supported Bilayers of Ternary Mixtures Containing Galactosylceramide. *Biophys. J.* **2008**, *94*, 2691−2697.
(43) Bischof, A. A.; Wilke, N. Molecular Determinants for the Line Tension of Coexisting Liquid Phases in Monolayers. *Chem. Phys. Lipids* **2012**, *165*, 737−744.
(44) Kariel, N.; Davidson, E.; Keough, K. M. Cholesterol Does Not Remove the Gel-Liquid Crystalline Phase Transition of Phosphatidylcholines Containing Two Polyenoic Acyl Chains. *Biochim. Biophys. Acta* **1991**, *1062*, 70−76.
(45) Mitchell, D. C.; Litman, B. J. Molecular Order and Dynamics in Bilayers Consisting of Highly Polyunsaturated Phospholipids. *Biophys. J.* **1998**, *74*, 879−891.
(46) Ackerman, D. G.; Feigenson, G. W. Multiscale Modeling of Four-Component Lipid Mixtures: Domain Composition, Size, Alignment, and Properties of the Phase Interface. *J. Phys. Chem. B* **2015**, *119*, 4240−4250.
(47) Heftberger, P.; Kollmitzer, B.; Rieder, A. A.; Amenitsch, H.; Pabst, G. In Situ Determination of Structure and Fluctuations of Coexisting Fluid Membrane Domains. *Biophys. J.* **2015**, *108*, 854−862.
(48) Rosetti, C.; Pastorino, C. Polyunsaturated and Saturated Phospholipids in Mixed Bilayers: a Study From the Molecular Scale to the Lateral Lipid Organization. *J. Phys. Chem. B* **2011**, *115*, 1002−1013.
(49) Perlmutter, J. D.; Sachs, J. N. Interleaflet Interaction and Asymmetry in Phase Separated Lipid Bilayers: Molecular Dynamics Simulations. *J. Am. Chem. Soc.* **2011**, *133*, 6563−6577.

DOI: 10.1021/acs.jpcb.6b10836
J. Phys. Chem. B 2017, 121, 1587−1600

(50) Bennun, S. V.; Hoopes, M. I.; Xing, C.; Faller, R. Coarse-Grained Modeling of Lipids. *Chem. Phys. Lipids* **2009**, *159*, 59−66.
(51) Almeida, P. F.; Vaz, W. L. C.; Thompson, T. E. Lateral Diffusion in the Liquid Phases of Dimyristoylphosphatidylcholine/Cholesterol Lipid Bilayers: A Free Volume Analysis. *Biochemistry* **1992**, *31*, 6739−6747.
(52) May, S.; BenShaul, A. Spontaneous Curvature and Thermodynamic Stability of Mixed Amphiphilic Layers. *J. Chem. Phys.* **1995**, *103*, 3839−3848.
(53) Collins, M. D.; Keller, S. L. Tuning Lipid Mixtures to Induce or Suppress Domain Formation Across Leaflets of Unsupported Asymmetric Bilayers. *Proc. Natl. Acad. Sci. U.S.A.* **2008**, *105*, 124−128.
(54) Blosser, M. C.; Honerkamp-Smith, A. R.; Han, T.; Haataja, M.; Keller, S. L. Transbilayer Colocalization of Lipid Domains Explained Via Measurement of Strong Coupling Parameters. *Biophys. J.* **2015**, *109*, 2317−2327.
(55) Putzel, G. G.; Uline, M. J.; Szleifer, I.; Schick, M. Interleaflet Coupling and Domain Registry in Phase-Separated Lipid Bilayers. *Biophys. J.* **2011**, *100*, 996−1004.
(56) Koldsø, H.; Shorthouse, D.; Hélie, J.; Sansom, M. S. P. Lipid Clustering Correlates with Membrane Curvature as Revealed by Molecular Simulations of Complex Lipid Bilayers. *PLoS Comput. Biol.* **2014**, *10*, No. e1003911.
(57) Galimzyanov, T. R.; Molotkovsky, R. J.; Bozdaganyan, M. E.; Cohen, F. S.; Pohl, P.; Akimov, S. A. Elastic Membrane Deformations Govern Interleaflet Coupling of Lipid-Ordered Domains. *Phys. Rev. Lett.* **2015**, *115*, No. 088101.
(58) Palmieri, B.; Yamamoto, T.; Brewster, R. C.; Safran, S. A. Line Active Molecules Promote Inhomogeneous Structures in Membranes: Theory, Simulations and Experiments. *Adv. Colloid Interface Sci.* **2014**, *208*, 58−65.
(59) Davis, R. S.; Sunil Kumar, P. B.; Sperotto, M. M.; Laradji, M. Predictions of Phase Separation in Three-Component Lipid Membranes by the MARTINI Force Field. *J. Phys. Chem. B* **2013**, *117*, 4072−4080.
(60) Risselada, H. J.; Marrink, S. J. The Molecular Face of Lipid Rafts in Model Membranes. *Proc. Natl. Acad. Sci. U.S.A.* **2008**, *105*, 17367−17372.
(61) Elliott, R.; Szleifer, I.; Schick, M. Phase Diagram of a Ternary Mixture of Cholesterol and Saturated and Unsaturated Lipids Calculated From a Microscopic Model. *Phys. Rev. Lett.* **2006**, *96*, No. 098101.
(62) Rawicz, W.; Olbrich, K. C.; McIntosh, T.; Needham, D.; Evans, E. Effect of Chain Length and Unsaturation on Elasticity of Lipid Bilayers. *Biophys. J.* **2000**, *79*, 328−339.
(63) Rajamoorthi, K.; Petrache, H. I.; McIntosh, T. J.; Brown, M. F. Packing and Viscoelasticity of Polyunsaturated Omega-3 and Omega-6 Lipid Bilayers as Seen by 2H NMR and X-ray Diffraction. *J. Am. Chem. Soc.* **2005**, *127*, 1576−1588.

DOI: 10.1021/acs.jpcb.6b10836
J. Phys. Chem. B 2017, 121, 1587−1600